




**Ferroelectric control of magnetic skyrmions in multiferroic heterostructures**Yu Wang,<sup>1,2</sup> Jiajun Sun,<sup>1,2</sup> Takahiro Shimada<sup>1,3</sup>,,<sup>3</sup> Hiroyuki Hirakata<sup>1,3</sup>,,<sup>3</sup> Takayuki Kitamura,<sup>3</sup> and Jie Wang<sup>1,2,\*</sup><sup>1</sup>*Department of Engineering Mechanics, Zhejiang University, Zheda Road 38, Hangzhou, Zhejiang 310027, China*<sup>2</sup>*Key Laboratory of Soft Machines and Smart Devices of Zhejiang Province, Zhejiang University,**Zheda Road 38, Hangzhou, Zhejiang 310027, China*<sup>3</sup>*Department of Mechanical Engineering and Science, Kyoto University, Kyoto-daigaku-Katsura, Nishikyo-ku, Kyoto 615-8540, Japan*

(Received 20 May 2020; accepted 6 July 2020; published 21 July 2020)

Magnetic skyrmions with a topological particle nature are considered as potential information carriers for future spintronics memory and logic devices. The stabilization of magnetic skyrmions at zero magnetic field in nanostructured components is a prerequisite for incorporating them into advanced nonvolatile memory devices. Here, using a real-space phase field model based on Ginzburg-Landau theory, we demonstrate that ferroelectric polarization can stabilize magnetic skyrmions at zero magnetic field in multiferroic heterostructures composed of MnSi, PbTiO<sub>3</sub>, and SrTiO<sub>3</sub>. The stabilization of magnetic skyrmions in multiferroic heterostructures essentially depends on the directions of spontaneous polarizations and the size ratios of different constituents, in which polarization-induced inhomogeneous strain plays an important role. By applying an electric field, the polarization switching takes place in the ferroelectric constituent and the polarization-induced strain changes in the multiferroic heterostructures, resulting in a transition from skyrmion to helical phase in the ferromagnetic constituent. In addition, the skyrmion and helical phases can coexist in the absence of an external field and be switched reversibly by a local magnetic field with a small magnitude. Stabilization and control of magnetic skyrmions by spontaneous polarization at zero magnetic field may create additional opportunities for nonvolatile skyrmion memory devices.

DOI: [10.1103/PhysRevB.102.014440](https://doi.org/10.1103/PhysRevB.102.014440)**I. INTRODUCTION**

Magnetic skyrmions are topologically protected vortexlike spin textures in a magnetic material with the Dzyaloshinskii-Moriya interaction (DMI) [1,2]. The formation of magnetic skyrmions is mainly determined by the delicate balance between the DMI and exchange interaction. The spontaneous magnetic skyrmion was first predicted theoretically in noncentrosymmetric ferromagnetic crystal [1]. Experimentally, magnetic skyrmions were observed in both bulk noncentrosymmetric MnSi crystals [2] and interfacial symmetry-broken thin films [3]. Due to their nanoscale size, topological protection, and low current density required for motion, skyrmions are promising for applications in high-density and low-power spintronic devices, which have drawn extensive attention in recent years [3–5]. For the application of skyrmions in nonvolatile memory devices, the prerequisite is to stabilize the skyrmions at zero magnetic field. In general, a ferromagnetic material with DMI often exhibits a spin spiral or helical ground state in the absence of a magnetic field [5,6]. When an intermediate magnetic field is applied, a periodic skyrmion lattice arises in the material before reaching the field-polarized ferromagnetic state at increased magnetic field. In most ferromagnetic materials, skyrmions can usually be stabilized only under an intermediate magnetic field and below or close to room temperature.

To stabilize skyrmions in a broad range of temperatures and with low or zero magnetic field, different approaches have been employed to suppress the helical states in ferromagnetic materials, such as laterally confined geometries [7], lateral magnetic fields [3], defects [8], current-induced spin-orbit torque [9], and electric field [10]. Due to the magnetoelastic coupling effect of ferromagnetic materials, elastic strain engineering has also become a promising approach to modulate topological magnetic structures and stabilize skyrmions in ferromagnetic materials [11]. For example, a strain induced by thermal mismatch can cause large anisotropic deformation of skyrmion lattices in an FeGe plate [12]. The uniaxial strain can modulate the skyrmion phase transitions in both MnSi bulk [13] and FeGa thin film [14]. In a magnetic nanostripe, strain can control the creation and propagation of skyrmions [15], or chop skyrmions from the helical phase [16]. In addition, the nonuniform strain distributions can provide the stability of skyrmions in a magnetic nanodot [17], nanostripe, and thin film [18]. By applying a nonuniform displacement to the surface of an FeGa thin film, Shi and Wang [18] predicted, from phase field simulations, that skyrmions can be stabilized by a nonuniform out-of-plane strain in the absence of an external magnetic field.

Engineering complicated strain distributions should be more promising to modulate the skyrmions in ferromagnetic materials, in contrast to the simple uniaxial and homogeneous strains that can only increase the stability of skyrmions in the presence of an external magnetic field. The skyrmions at zero magnetic field, as desired for application, can be stabilized by inhomogeneous strains in ferromagnetic materials [17,18].

\*jw@zju.edu.cn

The stabilization of skyrmions at zero magnetic field is highly dependent on the spatial distribution of the inhomogeneous strains. For the stabilization of skyrmion arrays, the periodic magnetization distribution in the materials may require a periodic strain distribution. Although the inhomogeneous strain has been demonstrated to stabilize the skyrmion array in ferromagnetic thin films [18], how to provide such an inhomogeneous and periodic strain in the materials at zero magnetic field has not been proposed yet. In particular, how to change the inhomogeneous and periodic strain in a controllable way, which is important for the control of skyrmions, is still unknown.

In this work, the spontaneous polarization of ferroelectrics is proposed to provide an inhomogeneous and wavelike strain in multiferroic heterostructures. Based on phase field simulations, we demonstrate that the spontaneous polarization in ferroelectric constituents can stabilize magnetic skyrmions in the ferromagnetic constituents at zero magnetic field in multiferroic heterostructures combining ferromagnetic MnSi, ferroelectric PbTiO<sub>3</sub>, and paraelectric SrTiO<sub>3</sub> constituents. The polarization-induced wavelike strains are found to play an important role in the stabilization of magnetic skyrmions in multiferroic heterostructures. By applying an electric field, polarization switching takes place in ferroelectric PbTiO<sub>3</sub> and the coincident polarization-related strain changes in the multiferroic heterostructures, resulting in a transition from skyrmion phase to helical phase in ferromagnetic MnSi. For the multiferroic thin films with out-of-plane spontaneous polarizations, the skyrmion and helical phases can coexist at zero magnetic field and can be switched reversibly by a local magnetic field, which makes them promising for application in spintronic devices based on topological magnetic structures.

## II. METHODOLOGY

A real-space phase field model based on Ginzburg-Landau theory is employed to investigate the evolution of the polarizations and magnetizations in multiferroic heterostructures. The polarizations and magnetizations are taken as the order parameters for ferroelectric and ferromagnetic constituents, respectively. The time-dependent Ginzburg-Landau (TDGL) equation is employed to describe the evolution of polarizations  $\mathbf{P}$  in the ferroelectric constituent as [19–21]

$$\frac{\partial \mathbf{P}}{\partial t} = -L_{\text{FE}} \frac{\delta F}{\delta \mathbf{P}}, \quad (1)$$

where  $L_{\text{FE}}$  is the kinetic coefficient and  $F$  is the total free energy. The total free energy can be expressed as  $F = \int f dv$ , where  $f$  represents the total free-energy density. The detailed formula of the total free-energy density for the multiferroic heterostructures with MnSi and PbTiO<sub>3</sub>/SrTiO<sub>3</sub> constituents is given in the Supplemental Material [22]. In general, the temporal evolution of magnetizations  $\mathbf{M}$  in ferromagnetic materials is described by the Landau-Lifshitz-Gilbert (LLG) equation as [18,23,24]

$$\frac{\partial \mathbf{M}}{\partial t} = -\gamma \mathbf{M} \times \mathbf{H}_{\text{eff}} + \frac{\alpha}{M_s} \mathbf{M} \times \frac{\partial \mathbf{M}}{\partial t}, \quad (2)$$

where  $\mathbf{H}_{\text{eff}} = \frac{-1}{\mu_0} \frac{\delta F}{\delta \mathbf{M}}$  is the effective magnetic field,  $\gamma$  is the gyromagnetic ratio, and  $\alpha$  is the Gilbert damping. With the

overdamped assumption [18,25–27], the LLG equation is reduced to the TDGL equation as

$$\frac{1}{L_{\text{FM}}} \frac{\partial \mathbf{M}}{\partial t} = -\frac{\delta F}{\delta \mathbf{M}}, \quad (3)$$

where  $L_{\text{FM}} = \frac{\gamma M_s}{\alpha \mu_0}$  is the kinetic coefficient for magnetization evolution [19]. In addition to the TDGL and LLG equations, the mechanical equilibrium equation,

$$\frac{\partial \sigma_{ij}}{\partial x_j} = \frac{\partial}{\partial x_j} \left( \frac{\partial f}{\partial \varepsilon_{ij}} \right) = 0, \quad (4)$$

and the Maxwell (or Gauss) equations,

$$\frac{\partial D_i}{\partial x_i} = \frac{\partial}{\partial x_i} \left( -\frac{\partial f}{\partial E_i} \right) = 0, \quad (5)$$

$$\frac{\partial B_i}{\partial x_i} = \frac{\partial}{\partial x_i} \left( -\frac{\partial f}{\partial H_i} \right) = 0, \quad (6)$$

must be satisfied for the stresses  $\sigma_{ij}$ , electric displacements  $D_i$ , and magnetic induction  $B_i$  in the multiferroic heterostructures, respectively. A nonlinear finite-element method is employed to solve the above governing equations. In the space discretization, an eight-node hexahedral element with 11 degrees of freedom at each node is employed. The degrees of freedom are three displacement components, one electrical potential, three polarization components, one magnetic potential, and three magnetization components. For the time integration, the backward Euler method is employed. The detailed procedure for solving these equations and the used material parameters are given in the Supplemental Material [22].

## III. RESULTS AND DISCUSSION

### A. Stable skyrmions in a multiferroic nanostripe

We first discuss the stabilization of skyrmions in a multiferroic nanostripe as shown in Fig. 1(a). In the multiferroic nanostripe, the upper layer is the chiral ferromagnetic material MnSi while the lower layer includes the alternative ferroelectric PbTiO<sub>3</sub> (PTO) and paraelectric SrTiO<sub>3</sub> (STO). The multiferroic nanostripe is assumed to be grown on a conductive substrate, so that the lower PTO/STO layer is under a short-circuited electrical boundary condition. A real-space phase field model of multiferroic heterostructures (see Sec. II) is employed to simulate the magnetization and polarization distributions in the upper and lower layers, respectively. Figure 1(b) shows the spatial distribution of polarization vectors obtained from the phase field simulation in the PTO/STO layer of the multiferroic nanostripe. It is found that polarizations in each PTO block form a single domain while polarizations in each STO block form an opposite single domain with a much smaller magnitude. Figure 1(c) gives the distribution of polarization components along the  $x_1$  direction in the middle plane of the PTO/STO layer. The polarization components  $P_1$  and  $P_2$  in both PTO and STO are trivial, whereas the polarization component  $P_3$  is nontrivial. The average magnitude of polarizations in PTO is 0.57 C/m<sup>2</sup> while it is less than 0.13 C/m<sup>2</sup> in STO. The small polarizations in STO are induced by the depolarization field of PTO because STO is an improper ferroelectric that has no polarization if there is no external field. The polarization direction of STO is opposite

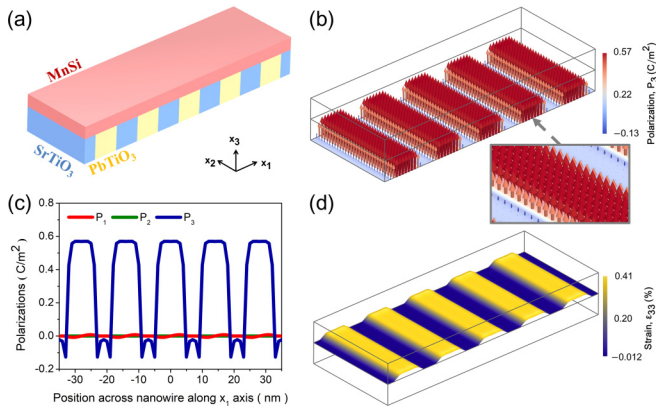


FIG. 1. (a) Schematic diagram of a multiferroic nanostripe constituted of  $\text{PbTiO}_3$ ,  $\text{SrTiO}_3$ , and  $\text{MnSi}$ . (b) The spatial distribution of polarization vectors obtained from phase field simulation in the PTO/STO layer of the multiferroic nanostripe. The polarizations in each PTO block form a single domain, while polarizations in each STO block form an opposite single domain with a much smaller magnitude. (c) The distribution of polarization components in the middle plane of the PTO/STO layer. The polarization components of  $P_1$  and  $P_2$  in both PTO and STO are trivial, whereas the polarization component  $P_3$  is nontrivial. (d) The wavelike strain induced by the wavelike polarizations in (c) due to the coupling between polarization and strain. This kind of wavelike strain is transferred into the upper  $\text{MnSi}$  layer via the coherent interface to stabilize the skyrmion phase.

to that of PTO, which is to reduce the total depolarization energy of the PTO/STO layer in the multiferroic nanostripe. The periodic wavelike polarizations in the PTO/STO layer generate a wavelike strain in Fig. 1(d) due to the coupling between polarization and strain. This kind of inhomogeneous and periodic strain is transferred into the upper  $\text{MnSi}$  layer via the coherent interface, which could stabilize the skyrmion phase in the  $\text{MnSi}$  layer. To stabilize the skyrmion phase in  $\text{MnSi}$ , the period of the wavelike strain should be comparable to the equilibrium period of the helical phase in  $\text{MnSi}$ , which is determined by the ratio of the DMI and exchange coupling coefficients. The period of the helical phase is about 14 nm

in  $\text{MnSi}$ , and so the period of the PTO/STO unit is taken as 14 nm in the present study.

On the other hand, the stability of the skyrmion phase is also dependent on the profile and magnitude of the wavelike strain, which is determined by the geometric configuration of the multiferroic nanostripe. To investigate the stability of skyrmions in the multiferroic nanostripe with different geometrical configurations, the phase diagram is constructed in terms of the width ratio of PTO and BTO and the thickness ratio of the ferromagnetic  $\text{MnSi}$  layer and the ferroelectric PTO/STO layer, as shown in Fig. 2(a). The horizontal axis represents the width ratio of PTO and STO, in which the total width of PTO and STO is fixed as 14 nm in one period along the  $x_1$  direction. The vertical axis denotes the thickness ratio of the ferromagnetic  $\text{MnSi}$  layer and the ferroelectric PTO/STO layer along the  $x_3$  direction, in which the thickness of the PTO/STO layer is fixed as 2 nm while the thickness of the  $\text{MnSi}$  layer varies. The width of the multiferroic nanostripe along the  $x_2$  direction is 28 nm. The phase diagram shows that there are two phases separated by the phase boundary in the  $\text{MnSi}$  layer. The insets of Fig. 2(a) show the simulated magnetization distributions in the skyrmions and helical phases, respectively. The skyrmions can be stable in the region where the width ratio of PTO/STO is large and the thickness ratio of FM/FE is small. When the  $\text{MnSi}$  layer becomes thick, the strain induced by the polarizations in PTO/STO is not enough to stabilize the skyrmions. It is interesting that 4/3 is the most favorable width ratio of PTO/STO to stabilize the skyrmions. Furthermore, temperature also plays an important role in the stability of magnetic topological structures [1,28,29]. To demonstrate the effect of temperature on the skyrmion state in the multiferroic nanostripe, a phase diagram in terms of temperatures and the thickness ratio of FM/FE is given in Fig. 2(b). The phase diagram shows that the temperature of 25 K near the Curie temperature of  $\text{MnSi}$  is the most favorable temperature to stabilize the skyrmion phase. Based on the phase diagrams of Figs. 2(a) and 2(b), the most favorable width ratio of PTO/STO and the temperature for stabilizing the skyrmion phase are 4/3 and 25 K, respectively, which are employed in all of the following simulations in the present study.

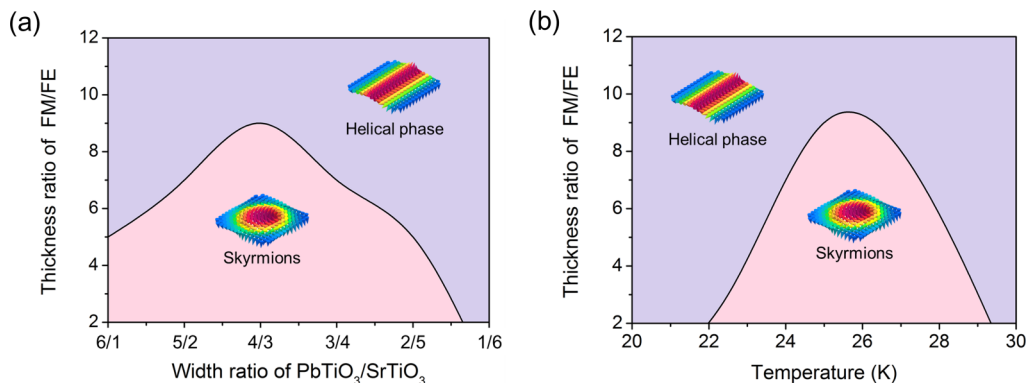


FIG. 2. (a) The phase diagram in terms of the width ratio of PTO and BTO and the thickness ratio of the ferromagnetic  $\text{MnSi}$  layer and the ferroelectric PTO/STO layer. There are two phases in the  $\text{MnSi}$  layer, and the insets show the simulated magnetization distributions of different phases. The skyrmion phase is stable in the region where the width ratio of PTO/STO is large and the thickness ratio of FM/FE is small. (b) The phase diagram in terms of temperatures and the thickness ratio of FM/FE. The temperature of 25 K near the Curie temperature of  $\text{MnSi}$  is the most favorable temperature to stabilize the skyrmion phase. In this phase diagram, the width ratio of the PTO/STO layer is set as 4/3.

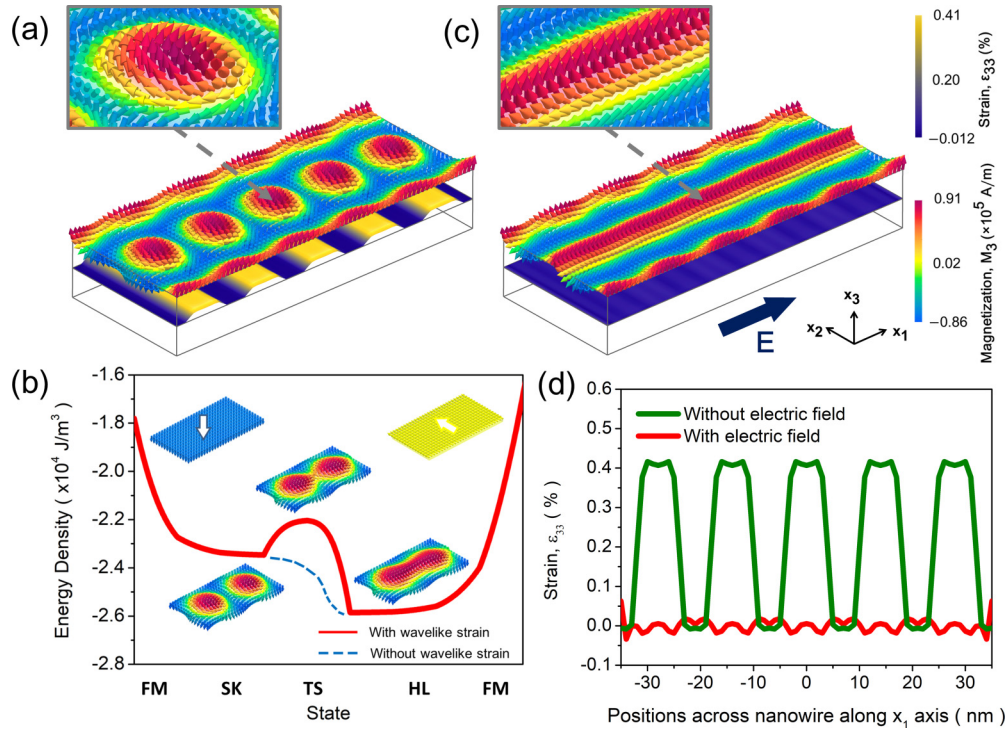


FIG. 3. (a) The stable magnetic skyrmion array emerges in the MnSi layer of a multiferroic nanostripe in the absence of external fields due to the wavelike strain in the below PTO/STO layer. (b) The energy profile of different magnetic states, in which FM, SK, TS, and HL denote the ferromagnetic, skyrmion, transient, and helical phases, respectively. The insets show the corresponding magnetization distributions in different phases. There is an energy barrier between the skyrmion and helical phases in the presence of the wavelike strain, which will disappear as the dashed line if the wavelike strain is absent. (c) The skyrmion phase loses its stability and evolves into the helical phase in the nanostripe when an in-plane electric field of  $E_1 = 5.7 \times 10^7$  V/m is applied in the  $x_1$  direction. (d) The strain distribution along the  $x_1$  axis in the nanostripe with and without the in-plane external electric field. The strain approaches zero when the electric field is applied, which makes the energy barrier in (b) disappear and the helical phase in (c) stable.

### B. Electrical control of the skyrmion phase transition

As we showed in the previous section, the skyrmions are stable in the absence of an external magnetic field in the MnSi layer subjected to a wavelike nonuniform strain generated by the periodic polarizations of the PTO/STO layer in multiferroic nanostripes. Figure 3(a) shows the simulated skyrmion array in a multiferroic nanostripe in the absence of an external magnetic field, in which the wavelike and nonuniform strain is also shown below the skyrmion array. The wavelike strain is the necessary condition for the stabilization of the skyrmion array in the multiferroic nanostripe. To reveal the underlying mechanism on the stable skyrmions in the absence of a magnetic field, the energy profile of different magnetization configurations with the wavelike strain is given in Fig. 3(b). The insets of Fig. 3(b) show the different magnetization configurations that correspond to the out-of-plane ferromagnetic, skyrmion, intermediate, helical, and in-plane ferromagnetic phases, respectively. The ferromagnetic phases with a single domain at the left and right side of the curve have relatively higher energy than the skyrmion and helical phases, which are unstable. The ferromagnetic phase with the out-of-plane and in-plane magnetizations will evolve to the skyrmion and helical phases, respectively, to reduce the energy. Although the skyrmion phase has a higher energy than the helical phase, it cannot evolve to the helical phase spontaneously

because there is an energy barrier between these two phases. The magnitude of the energy barrier between the skyrmion and helical phases depends on the amplitude of the wavelike strain. Shi and Wang [18] predicted that the energy barrier will disappear when the wavelike strain is less than a threshold.

Although the skyrmion phase can be stable in the nanostripe in the absence of an external magnetic field, it is a metastable phase according to the energy profile in Fig. 3(b). The metastable skyrmion phase will become the more stable helical phase if the energy barrier is removed by reducing the wavelike strain. To reduce the wavelike strain in the multiferroic nanostripe, an in-plane electric field of  $E_1 = 5.7 \times 10^7$  V/m is applied in the  $x_1$  direction to switch the polarizations from out-of-plane to in-plane. The polarization switching induced by the electric field leads to the elimination of the wavelike strain in the MnSi layer, as shown in Fig. 3(d). Without the wavelike strain, the energy barrier between the skyrmion and helical phases disappears, as shown by the dashed line in Fig. 3(b). Hence, the skyrmion phase loses its stability and evolves into the helical phase, as shown in Fig. 3(c). The detailed process of the phase transitions driven by the electric field in the multiferroic nanostripe is given by Fig. S1 in the Supplemental Material [22]. When the electric field is removed, the polarizations will switch back to out-of-plane due to the depolarization field in PTO and the wavelike strain appears again. The helical phase is stable even under

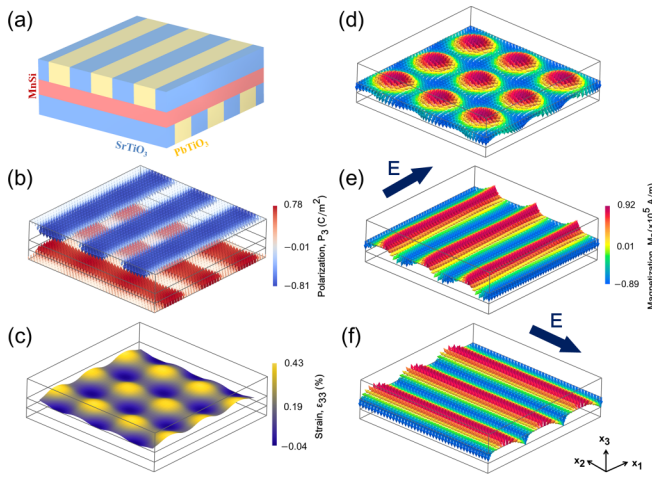


FIG. 4. (a) The schematic diagram of a sandwiched multiferroic thin film with orthogonal PTO/STO layers. (b) The spontaneous polarizations form single domains with orientations along the  $x_3$  negative and positive directions in the top and bottom PTO/STO layers, respectively. (c) The chessboard-like strain in the MnSi layer generated by the orthogonal wavelike polarizations in the top and bottom PTO/STO layers via the electrostriction effect. (d) The stable skyrmion lattices appear in the MnSi layer of the multiferroic thin film at zero magnetic field due to the chessboard-like strain. (e),(f) The skyrmion lattices evolve into different helical phases when in-plane electric fields are applied along the  $x_1$  and  $x_2$  directions, respectively.

the wavelike strain due to the lower energy. The ferromagnetic phase with out-of-plane magnetization can be obtained from the helical phase if an out-of-plane magnetic field is applied. When the magnetic field is removed, the unstable ferromagnetic phase evolves to the metastable skyrmion phase. As a result, the metastable skyrmion phase and the stable helical phase can be switched back and forth by applying an in-plane electric field and an out-of-plane magnetic field, respectively. The two phases can be stable in the absence of an external field, which are nonvolatile and useful for applications in spintronic devices.

### C. Skyrmion phase transition in a multiferroic thin film

Next, we investigate the electrical control of the skyrmion phase transition in a multiferroic thin film, as shown in Fig. 4(a). The multiferroic thin film is a sandwich structure, in which the bottom and top layers are two orthogonally arranged PTO/STO composite thin films while the middle layer is a MnSi thin film. The thicknesses of the MnSi layer and the bottom and top PTO/STO layers are 2, 2, and 5 nm, respectively. The widths of PTO and STO in the PTO/STO layers are 8 and 6 nm, respectively. The periodic boundary conditions are employed in the  $x_1$  and  $x_2$  directions of the simulated thin film. In the simulation, the displacement  $u_3$  in the  $x_3$  direction of the bottom surface is fixed. The traction-free mechanical boundary condition is set to the top surface. The “open-circuit” magnetic boundary conditions are set on the interface. The short-circuit electrical boundary conditions are set on the top and bottom surfaces and the MnSi layer. Similar to that of the nanostripes, the spontaneous polarizations in

PTOs of thin films form single domains with orientations along the  $x_3$  negative and positive directions in the top and bottom PTO/STO layers, respectively, as shown in Fig. 4(b). The top and bottom PTO/STO layers exhibit orthogonal wavelike polarizations, which generate a chessboard-like strain in the MnSi layer via the electrostriction effect, as shown in Fig. 4(c). With this chessboard-like strain, the stable skyrmion lattices appear in the MnSi layer of the multiferroic thin film at zero magnetic field, as shown in Fig. 4(d). It should be noted that the skyrmion lattice is stable in the absence of any external field, which is also nonvolatile.

The skyrmion lattice in the multiferroic thin film can also be controlled by an electric field. In Figs. 4(e) and 4(f), the in-plane electric fields are applied in the top and bottom PTO/STO layers. The initial skyrmion lattices evolve into the helical phase when in-plane electric fields are applied along the  $x_1$  and  $x_2$  directions, respectively. It is found that the directions of the helical stripes are always along the directions of the in-plane electric field. In the process of a phase transition, the direction of the polarizations in the ferroelectric PTO is switched from out-of-plane to along the external electric field. Hence, the chessboard-like strain disappears and a tensile strain along the direction of the external electric field appears in the multiferroic thin film due to the electrostriction effect. With the disappearance of the chessboard-like strain, the skyrmion lattices lose their stability and evolve into helical phases along the easy axis resulting from the tensile strain. The detailed process of the skyrmion phase transitions in a multiferroic thin film are given by Fig. S2 in the Supplemental Material [22]. After removing the in-plane electric field and applying an out-of-plane magnetic field, the helical phase becomes a ferromagnetic phase with a single domain, which can evolve to a skyrmion lattice again when the magnetic field is removed. The switchable property between the skyrmion and helical phases has potential applications in microwave diode devices [30]. In addition, the specific-heat capacity of skyrmions is larger than that of the helical phase [31], which makes heat conduction quicker in helical stripes than skyrmions lattices. The direction of heat conduction can be controlled by changing the direction of the helical phase though an electric field, which is useful for nanoscale directional heat conduction devices.

### D. Coexistence of skyrmion and helical phases

In previous sections, we have shown that both skyrmions and helical phases are stable with the polarization-induced nonuniform strain in the multiferroic heterostructures in the absence of magnetic fields. The existence of an energy barrier in the energy profile of Fig. 3(b) implies that the skyrmion and helical phases may coexist stably. To verify this expectation, the  $3 \times 3$  skyrmion lattices of Fig. 4(d) have been enlarged to the  $6 \times 6$  skyrmion lattices as shown in Fig. 5(a) by doubling the in-plane size of the multiferroic thin film of Fig. 4(a). Although the transition from the skyrmion phase to the helical phase occurs from Figs. 4(d) to 4(e), the coexistence of the skyrmion and helical phases in the multiferroic thin films does not occur because all skyrmions are transferred to the helical phase under the uniform in-plane electric field. To realize

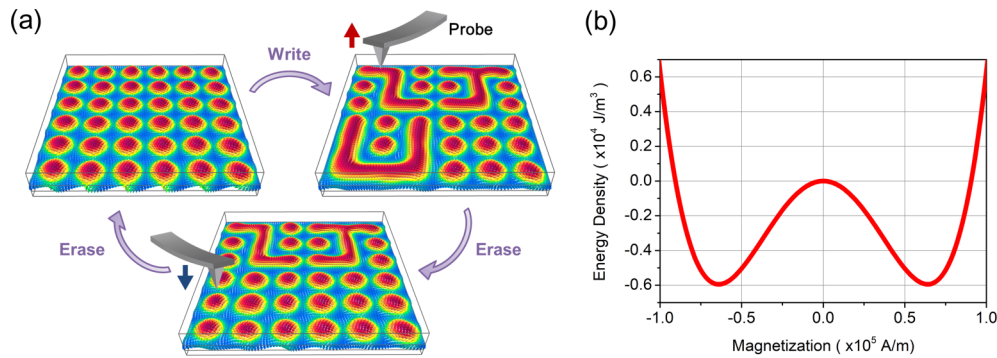


FIG. 5. (a) The writing and erasing process of the helical stripe by the local magnetic field of MFM probe tip in the skyrmion lattices of a multiferroic thin film, in which the skyrmions and helical stripe can coexist in the absence of magnetic field. The different helical stripes can be used as information carriers, which have potential application in storage devices. (b) The double-well potential for common ferromagnetic MnSi domains with different orientations and magnitudes. The energy barrier between two opposite domains is three times larger than that between the skyrmions and helical phases in Fig. 3(b), suggesting that the energy consumption of data writing will be lower in the present multiferroic thin films than that of traditional devices with domains as information carriers.

the coexistence of the skyrmion and helical phases, a local magnetic field of  $H_3 = 1.56 \times 10^4$  A/m in the  $x_3$  direction is applied at the gap between two skyrmions, which connects the adjacent skyrmions to form a helical stripe. The helical stripe can be stable in the skyrmion lattice after the local magnetic field is removed. In practice, the local magnetic field could be applied by a saturated magnetic probe of a magnetic force microscope (MFM). When the magnetic probe scans above the skyrmion lattice, different helical stripes can be written in the skyrmion lattice, as shown by the letters “ZJU” in Fig. 5(a). The written letters can be stable without any external field, which is nonvolatile and can be employed as an information carrier. To erase the information, an opposite local magnetic field can be applied by the magnetic probe to disconnect the helical stripe into isolated skyrmions, as shown by the lower part of Fig. 5(a), in which the letter “U” is deleted by the magnetic probe. The remained letters “ZJ” are still stable and unchanged without an external field after the probe is removed. When all the letters are deleted, the thin film recovers its initial state with skyrmion lattices. The procedures of writing and erasure are repeatable and can be controlled by a computer program, which makes the patterns programmable in the thin film.

Due to the nanoscale size, the information devices based on skyrmions could have an ultrahigh density compared to traditional domain-based information devices. Furthermore, the energy barrier between the skyrmion phase and helical phase is much smaller than that between the common ferromagnetic domains with opposite orientations. Figure 5(b) shows the double-well potential for common ferromagnetic domains with different orientations and magnitudes. Two minimum points in the double-well potential correspond to two stable domains with opposite magnetization orientations, which are used as nonvolatile information carriers in traditional ferromagnetic data-storage devices. The energy barrier between two opposite domains is around  $6.0 \times 10^3$  J/m<sup>3</sup> in Fig. 5(b), which is three times larger than the energy barrier of  $1.9 \times 10^3$  J/m<sup>3</sup> between the skyrmion phase and the helical phase in Fig. 3(b). These results show that the energy consumption of writing data in the storage devices

will decrease significantly if the skyrmion and helical phases of the present multiferroic thin films are employed as nonvolatile information carriers to replace the traditional domain-based information carriers. Furthermore, the energy barrier in Fig. 3(b) could be reduced by decreasing the amplitude of the wavelike strain in the thin films [18], which further reduces the energy consumption. The skyrmion and helical phases in the present multiferroic thin films are nonvolatile, programmable, switchable, and they require low energy consumption for writing information, hence they may be applicable for nonvolatile memory devices based on topological magnetic structures.

#### IV. CONCLUSIONS

In summary, we have investigated the stabilization and phase transition of magnetic skyrmions in multiferroic heterostructures from phase field simulations. Two kinds of multiferroic heterostructures with a periodic distribution of spontaneous polarization are proposed to stabilize the skyrmion phase in the ferromagnetic constituent of MnSi in the absence of a magnetic field. The stabilization of skyrmions in the ferromagnetic constituents is attributed to a wavelike strain, which is generated by the spontaneous polarizations in ferroelectric constituents via electrostriction.

The detailed energy analysis shows that the skyrmion phase is metastable under wavelike strain. When an in-plane electric field is applied to the ferroelectric constituent of multiferroic heterostructures, the spontaneous polarizations switch from out-of-plane to in-plane, and thus the wavelike strain disappears, resulting in a transition from the skyrmion phase to the helical phase in ferromagnetic constituents. After removing the electric field, the helical phase is stable even under wavelike strain because it has a lower energy than the skyrmion phase. The stable helical phase can return to the metastable skyrmion phase via the intermediate ferromagnetic phase induced by an out-of-plane magnetic field.

For multiferroic thin films with out-of-plane spontaneous polarizations, the skyrmion and helical phases can coexist in the absence of an external magnetic field, which can be switched from one to the other through a local magnetic field

generated by a probe of a magnetic force microscope. The skyrmion and helical phases in multiferroic thin films exhibit several excellent properties, including being nonvolatile, programmable, switchable, and having lower energy consumption for phase transformation, thus they may be applicable in future spintronic devices with ultrahigh density and low energy consumption.

## ACKNOWLEDGMENTS

This work was financially supported by the National Natural Science Foundation of China (Grants No. 11672264 and No. 11972320) and Zhejiang Provincial Natural Science Foundation (Grant No. LZ17A020001).

The authors declare no conflict of interest.

- 
- [1] U. K. Rößler, A. N. Bogdanov, and C. Pfleiderer, *Nature (London)* **442**, 797 (2006).
- [2] S. Mühlbauer, B. Binz, F. Jonietz, C. Pfleiderer, A. Rosch, A. Neubauer, R. Georgii, and P. Böni, *Science* **323**, 915 (2009).
- [3] X. Z. Yu, Y. Onose, N. Kanazawa, J. H. Park, J. H. Han, Y. Matsui, N. Nagaosa, and Y. Tokura, *Nature (London)* **465**, 901 (2010).
- [4] R. Wiesendanger, *Nat. Rev. Mater.* **1**, 16044 (2016).
- [5] G. Finocchio, F. Büttner, R. Tomasello, M. Carpentieri, and M. Kläui, *J. Phys. D* **49**, 423001 (2016).
- [6] C. Kittel, *Introduction to Solid State Physics* (Wiley, New York, 1976) pp. 155-181.
- [7] C. Jin, Z. A. Li, A. Kovács, J. Caron, F. Zheng, F. N. Rybakov, N. S. Kiselev, H. Du, S. Blügel, M. Tian, Y. Zhang, M. Farle, and R. E. Dunin-Borkowski, *Nat. Commun.* **8**, 15569 (2017).
- [8] S.-Z. Lin, C. Reichhardt, C. D. Batista, and A. Saxena, *Phys. Rev. B* **87**, 214419 (2013).
- [9] W. Jiang, P. Upadhyaya, W. Zhang, G. Yu, M. B. Jungfleisch, F. Y. Fradin, J. E. Pearson, Y. Tserkovnyak, K. L. Wang, O. Heinonen, S. G. E. Te Velthuis, and A. Hoffmann, *Science* **349**, 283 (2015).
- [10] Y. Okamura, F. Kagawa, S. Seki, and Y. Tokura, *Nat. Commun.* **7**, 12669 (2016).
- [11] J. Wang, *Annu. Rev. Mater. Res.* **49**, 361 (2019).
- [12] K. Shibata, J. Iwasaki, N. Kanazawa, S. Aizawa, T. Tanigaki, M. Shirai, T. Nakajima, M. Kubota, M. Kawasaki, H. S. Park, D. Shindo, N. Nagaosa, and Y. Tokura, *Nat. Nanotechnol.* **10**, 589 (2015).
- [13] Y. Nii, T. Nakajima, A. Kikkawa, Y. Yamasaki, K. Ohishi, J. Suzuki, Y. Taguchi, T. Arima, Y. Tokura, and Y. Iwasa, *Nat. Commun.* **6**, 8539 (2015).
- [14] J. Wang, Y. Shi, and M. Kamlah, *Phys. Rev. B* **97**, 024429 (2018).
- [15] Z. Li, Y. Zhang, Y. Huang, C. Wang, X. Zhang, Y. Liu, Y. Zhou, W. Kang, S. C. Koli, and N. Lei, *J. Magn. Magn. Mater.* **455**, 19 (2018).
- [16] Y. Liu, N. Lei, W. Zhao, W. Liu, A. Ruotolo, H.-B. Braun, and Y. Zhou, *Appl. Phys. Lett.* **111**, 022406 (2017).
- [17] J.-M. Hu, T. Yang, and L.-Q. Chen, *npj Comput. Mater.* **4**, 62 (2018).
- [18] Y. Shi and J. Wang, *Phys. Rev. B* **97**, 224428 (2018).
- [19] J. Wang and J. Zhang, *Int. J. Solids Struct.* **50**, 3597 (2013).
- [20] L. Van Lich, T. Shimada, K. Miyata, K. Nagano, J. Wang, and T. Kitamura, *Appl. Phys. Lett.* **107**, 232904 (2015).
- [21] L. Van Lich, T. Shimada, K. Nagano, Y. Hongjun, J. Wang, K. Huang, and T. Kitamura, *Acta Mater.* **88**, 147 (2015).
- [22] See the Supplemental Material at <http://link.aps.org/supplemental/10.1103/PhysRevB.102.014440> for details of the Figs. S1 and S2, the phase field model, the finite-element method, and the material parameters.
- [23] S. Zhang and Z. Li, *Phys. Rev. Lett.* **93**, 127204 (2004).
- [24] J. Iwasaki, M. Mochizuki, and N. Nagaosa, *Nat. Nanotechnol.* **8**, 742 (2013).
- [25] A. Gordon, I. D. Vagner, and P. Wyder, *Phys. Rev. B* **41**, 658 (1990).
- [26] Y. Ni, L. He, and A. G. Khachatryan, *J. Appl. Phys.* **108**, 023504 (2010).
- [27] X. Lu, H. Li, and B. Wang, *J. Mech. Phys. Solids* **59**, 1966 (2011).
- [28] Y. Hu and B. Wang, *New J. Phys.* **19**, 123002 (2017).
- [29] A. O. Leonov and A. N. Bogdanov, *New J. Phys.* **20**, 043017 (2018).
- [30] M. Mochizuki and S. Seki, *Phys. Rev. B* **87**, 134403 (2013).
- [31] A. Bauer, M. Garst, and C. Pfleiderer, *Phys. Rev. Lett.* **110**, 177207 (2013).